Asociación Argentina
de Mecánica Computacional

Mecánica Computacional Vol XXX, págs. 2289-2300 (artículo completo)
Oscar Möller, Javier W. Signorelli, Mario A. Storti (Eds.)
Rosario, Argentina, 1-4 Noviembre 2011

# HEAT TRANSFER MODELING FOR PERTURBED TURBULENT FLOW

**Hugo D. Pasinato**

*Departamento de Ing. Química, FRN-Universidad Tecnológica Nacional, Avda. P. Rotter s/n, 8318 Plaza Huincul, Argentina; hpasinato@frn.utn.edu.ar; Tel. +54-299-4960510; Fax. +54-299-4963292*

**Keywords:** Velocity-temperature dissimilarity, Turbulent heat transfer, Bounded turbulent flow, Direct numerical simulation.

**Abstract.** A wall-layer turbulent heat transfer model based on turbulent momentum flux is proposed. A pre-generated database obtained from a direct numerical simulation of the perturbed turbulent channel and plane Couette flows with heat transfer was used. Local blowing and suction, axial and wall-normal pressure gradient steps, and a local wall temperature step were used as perturbations in these turbulent flows for both configurations. The turbulent heat fluxes were modeled based on a transformation of the turbulent fluxes by the mean wall-normal gradient of the temperature and axial velocity. *A priori* comparisons show that the model performs well for the type of perturbed turbulent flow and configurations used in this study.

## 1 INTRODUCTION

In the last decade, the prediction of turbulent heat transfer has received a significant amount of attention because turbulent heat transfer modeling had been outdated in relation to the actual computational capacity. Due to the difficulty involved in experimentally studying turbulent heat transfer, many previous works have employed direct numerical simulation (DNS), large eddy simulation (LES), and Reynolds-averaged Navier Stokes (RANS) approximations (Kim and Moin, 1989; Kasagi and Nishimura, 1997; Lyons et al, 1991; Abe and Suga, 2001; Houra and Nagano, 2006; Qiu et al, 2008; Rossi and Iaccarino, 2009; Rossi, 2010). Several published studies on turbulent heat transfer modeling use the standard gradient-diffusion hypothesis, in which the turbulent scalar fluxes are assumed to be proportional to the mean scalar gradient. However, this assumption has significant limitations, mainly in the prediction of the axial turbulent flux. An early alternative to this hypothesis was the generalized gradient-diffusion hypothesis proposed by Daly and Harlow (1970), in which the eddy diffusivity is calculated as a function of the Reynolds stress. In addition, Kim and Moin (1989), in a numerical study on scalar transport based on the analysis of DNS data of heat transfer in a turbulent channel flow, suggested using the Reynolds stress to predict the turbulent scalar fluxes. For instance, in the past, the similarity/dissimilarity between the velocity and the temperature was investigated in studies on turbulence, as researchers sought a new finding that could improve turbulent heat transfer modeling. Recently, a new type of study has been applied to turbulent heat transfer, addressing the velocity and temperature dissimilarity in perturbed turbulent flows (Suzuki et al., 1988; Suzuki and Inaoka, 1998; Kong et al., 2001; Pasinato, 2011a; Pasinato and Squires, 2011). In Pasinato (2011a) and Pasinato and Squires (2011), the dissimilarity between a developed and perturbed turbulent flow with heat transfer was numerically studied using DNS. The main goal of these studies was to create a DNS data set and study the velocity and temperature dissimilarity with respect to heat transfer modeling. In Pasinato (2011a), it was found that the natural dissimilarity between the fluctuation of the axial velocity, $u'$, and the temperature, $\theta'$, was due to a stronger correlation between $\theta'$ and the axial gradient of the instantaneous pressure, $\partial p'/\partial x$, as compared to $u'$ and $\partial p'/\partial x$. In Pasinato and Squires (2011), it was shown that the dissimilarity between the Reynolds stress and the turbulent heat flux is strongly dependent on the wall-normal gradient of the mean field dissimilarity and the velocity-pressure gradient interaction. However, most importantly, mean field modifications always play a fundamental role in heat and Reynolds stress dissimilarity.

In the present work, a relation involving $u'$, $\theta'$, the wall-normal gradient of the mean axial velocity, $(\partial U/\partial y)$, and the temperature, $(\partial \Theta/\partial y)$, is presented, which can be used to formulate a strategy for wall-layer turbulent heat transfer prediction. (Note that, throughout this work, the expression *mean field dissimilarity* will be used for the difference $\Phi = (U - \Theta)$ in dimensionless form, where $U$ and $\Theta$ are the mean axial velocity and temperature, respectively; *dissimilarity of the axial velocity and temperature fluctuations* for the dimensionless difference $\phi' = (u' - \theta')$; *axial turbulent flux dissimilarity* for the dimensionless difference $(\langle u'u' \rangle - \langle \theta'u' \rangle)$; and *wall-normal turbulent flux dissimilarity* for the dimensionless difference $(\langle u'v' \rangle - \langle \theta'v' \rangle)$). This proposal is based on previous works examining dissimilarity in perturbed flows with heat transfer. A DNS database generated from these previous works for developed and perturbed turbulent channel and plane Couette flows with heat transfer is used. The perturbations include local blowing or suction from a narrow span-wise slot at the walls, a local axial adverse pressure gradient step, an axial favorable pressure gradient step in a narrow span-wise volume in the buffer region, a local wall-normal pressure gradient, and a local wall temperature step.

In the next section, the fundamental aspects of dissimilarity in the wall layer are discussed, and a relation between $u_{rms}$, $\theta_{rms}$, the mean wall-normal gradient of $U$, and $\Theta$ is proposed. In section 3, a model for the turbulent heat flux based on the Reynolds stress and an *a priori* comparison of this model are presented. Finally, in the last section, some conclusions are drawn.

## 2 THE FUNDAMENTALS OF DISSIMILARITY IN PERTURBED TURBULENT FLOW

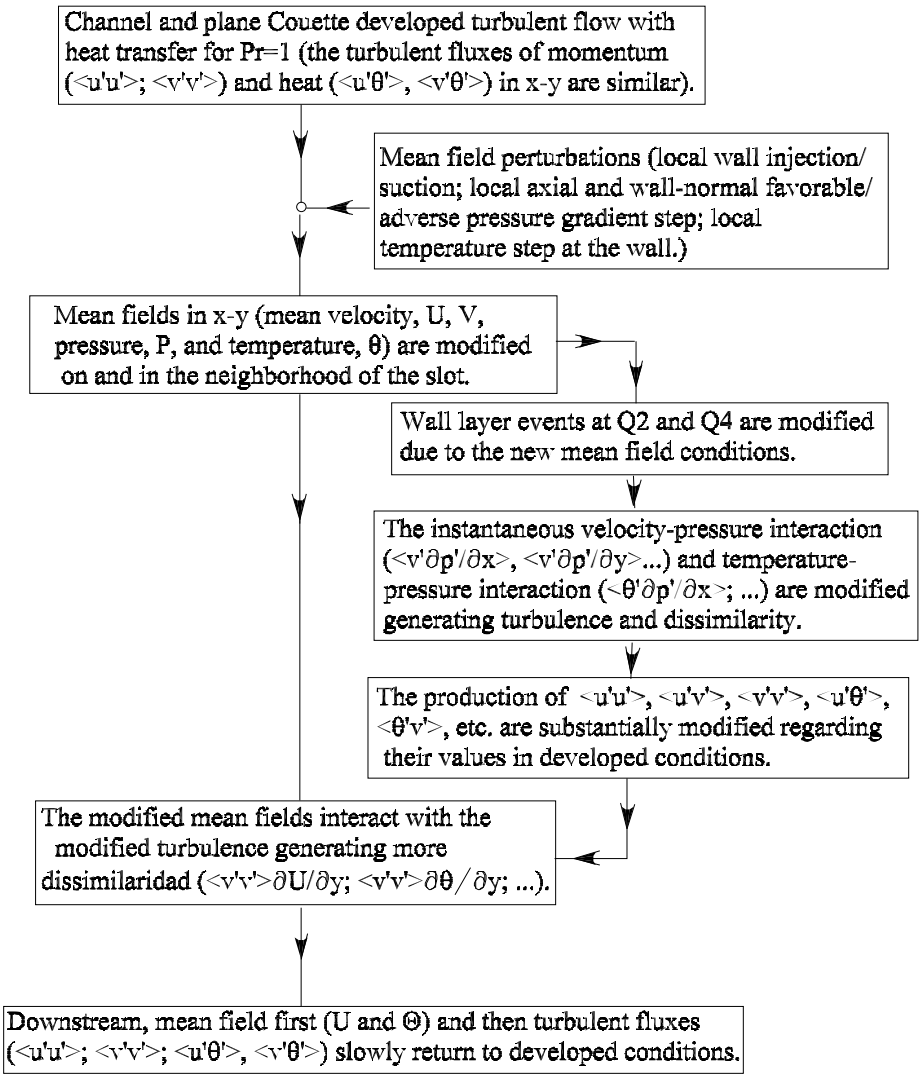


Figure 1: Representative diagram of the dissimilarity process between the Reynolds stress and the turbulent heat flux in the *x*-*y* plane.

The main conclusion from Pasinato and Squires (2011) is that dissimilarity between the Reynolds stress and the turbulent heat flux is strongly dependent on the interaction of the mean field gradient and the second moments of the velocity fluctuations, as well as on the velocity- and temperature-pressure interactions. On the mean field, most of the dissimilarity is generated by the wall-normal gradient of the mean dissimilarity $(\partial(U-\Theta)/\partial y)$. On the turbulence second velocity moments, on the other hand, most of the dissimilarity is generated by $\langle v'v'\rangle$ and $\langle u'v'\rangle$. And, on the velocity and pressure interaction, most of the dissimilarity is generated by $\langle v'\partial p'/\partial x\rangle$. Additionally, the term $\langle v'\partial p'/\partial y\rangle$ plays a fundamental role in generating $\langle v'v'\rangle$;

| | Non-perturbed | On slot | $W^+$ | $5W^+$ |
|---|---|---|---|---|
| $\langle\phi'\partial p'/\partial x\rangle$ | -0.0254 | -0.0513 | -0.1825 | -0.0435 |
| $\langle u'\partial p'/\partial x\rangle$ | 0.0209 | 0.0315 | 0.1368 | 0.0384 |
| $\langle\theta'\partial p'/\partial x\rangle$ | 0.0463 | 0.0828 | 0.3193 | 0.0819 |
| $\langle\phi'\partial p'/\partial y\rangle$ | 0.0195 | 0.0292 | 0.1295 | 0.0338 |
| $\langle\phi'\partial p'/\partial y\rangle_{(Q2+Q4)}$ | 0.0143 | 0.0157 | 0.0950 | 0.0286 |
| $\langle u'\partial p'/\partial y\rangle$ | -0.0242 | -0.0106 | 0.0463 | -0.0276 |
| $\langle\theta'\partial p'/\partial y\rangle$ | -0.0437 | -0.0397 | -0.0832 | -0.0614 |
| $\langle v'\partial p'/\partial x\rangle$ | -0.0171 | -0.0219 | -0.1819 | -0.0471 |
| $\langle v'\partial p'/\partial x\rangle_{(Q2+Q4)}$ | -0.0141 | -0.0175 | -0.1373 | -0.0363 |
| $\langle v'\partial p'/\partial y\rangle$ | -0.0112 | -0.0317 | -0.0874 | -0.0079 |
| $\langle v'\partial p'/\partial y\rangle_{(Q2+Q4)}$ | -0.0026 | -0.0170 | -0.0661 | 0.0008 |

Table 1: pressure-velocity interaction for channel flow at $y^+ = 38$ perturbed with blowing. Non-dimensionalization with $u_\tau^4/\nu$ and $T_\tau u_\tau^3/\nu$.

thus, it also plays an important role in the dissimilarity of the Reynolds stress and turbulent heat flux. Finally, it can be shown (Pasinato, 2011a,b) that the main source of the dissimilarity variance, $\phi'^2 = (u' - \theta')^2$, is the production term $(\langle u'v'\rangle - \langle\theta'v'\rangle)(\partial U/\partial y - \partial\Theta/\partial y)$ or $\langle\phi'v'\rangle(\partial\Phi/\partial y)$. This last production term implies that the variance of the difference between $u'$ and $\theta'$ depends on the dissimilarity of the wall-normal turbulent flux and on the wall-normal gradient of the mean fields.

Figure 1 presents a diagram of the dissimilarity process under the effects of mean field perturbations. In this figure, a former developed turbulent flow with a heat transfer with $Pr = 1$ is perturbed. In the former developed turbulent flow, the Reynolds stress and the turbulent heat fluxes were similar. However, near the slot, the mean flow and thermal field are substantially modified and are not similar due to the modification of the mean pressure field. The mean pressure field also affects the turbulence field through $U$ and $\Theta$. First, the level of the mean axial momentum and heat at the center and the wall layer suffer some differential modifications (due to the mean pressure field) as regarding they values in developed conditions. For instance, the events at $Q2$ (which, according to the turbulence *quadrant analysis*, is a combination of $v' > 0$ and $u' < 0$) and $Q4(v' < 0$ with $u' > 0)$, which are responsible for the wall-normal turbulence transfer between the wall layer and the central region, are substantially modified. The most important modification is the increased interaction $\langle v'\partial p'/\partial x\rangle$, which basically occurs at the $Q2$ and $Q4$ events. In these velocity-pressure interactions, the level of the correlation between $v'$ and $\nabla p'$ is of fundamental importance in the $\langle v'\theta'\rangle$ and $\langle v'u'\rangle$ dissimilarity, and in the variance production of $\phi'$. The second moments $\langle u'\partial p'/\partial x\rangle$ and $\langle\theta'\partial p'/\partial x\rangle$ also undergo important modifications, but they mostly maintain the relation $2\langle u'\partial p'/\partial x\rangle \simeq \langle\theta'\partial p'/\partial x\rangle$ as in a developed turbulent flow. Therefore, these correlations are not relevant to the generation of dissimilarity for the type of perturbations used in this study. Thus, the leading terms producing dissimilarity in the turbulent flux for the overall process are $\langle v'v'\rangle\partial\Phi/\partial y$ and $\langle v'\partial p'/\partial x\rangle$. Otherwise, the term $\langle v'\partial p'/\partial y\rangle$ is relevant in producing $\langle v'v'\rangle$, and the leading term in producing the dissimilarity variance is $\langle\phi'v'\rangle\partial\Phi/\partial y$ (Pasinato, 2011b).

The above description gives a broad picture of the dissimilarity process. However, there are interesting details regarding how the mean pressure field affects the turbulence production. Figures 2(a) and 2(b) show the axial distribution of $\langle v'v'\rangle^+$, $\langle u'v'\rangle^+$, $\langle\theta'v'\rangle^+$, $\langle v'\partial p'/\partial x\rangle^+$, and $\langle v'\partial p'/\partial y\rangle^+$ as well as of the mean field pressure $P^+$. These figures clearly show the importance

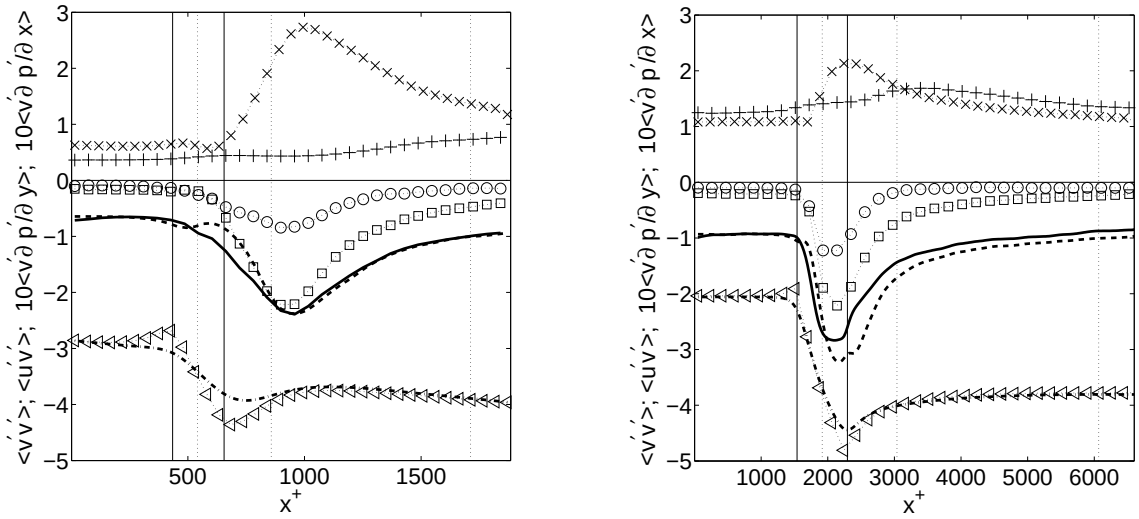


(a) (b)

Figure 2: Importance of wall-normal velocity-pressure interaction on $\langle v'u' \rangle$ and $\langle v'\theta' \rangle$ dissimilarity for perturbed flow with blowing. $\times \cdot \times \cdot \times$ and $+ \cdot + \cdot +$, $\langle v'v' \rangle^+$ at $y^+ \simeq 38$ and 137, respectively; $- - -$, $\langle u'v' \rangle^+$; solid line, $\langle \theta'v' \rangle^+$;$\circ \cdot \circ \cdot \circ$ , $10\langle v'\partial p'/\partial y \rangle^+$; $\square \cdot \square \cdot \square$, $10\langle v'\partial p'/\partial x \rangle^+$ at $y^+ \simeq 38$; $\triangleright \cdot \triangleright \cdot \triangleright$, and $-. - .-$, $0.05 \times P^+ - 3.5$ at $y^+ \simeq 38$ and 137, respectively. (a) Channel and (b) Couette flow.

of the velocity-pressure interaction terms for the $\langle v'u' \rangle$ and $\langle v'\theta' \rangle$ dissimilarity, although they are not the leading terms. There is a complete agreement between the location at which this dissimilarity arises, at approximately $x^+ \simeq 500$, and the point at which the velocity-pressure interaction terms increase significantly. They also show how the velocity-pressure interaction terms are related to the slightly adverse mean pressure gradient at the central region and wall layer, which is higher near the wall. As stated above, there is a differential mean pressure gradient that causes a modification of the turbulence field through the intensity of the events at $(Q2 + Q4)$, as shown below.

Table 1 shows that an important part of the correlations $\langle v'\partial p'/\partial x \rangle^+$ and $\langle v'\partial p'/\partial y \rangle^+$ are generated at the $(Q2 + Q4)$ events. In this table, the total as well as the part generated by the events at $(Q2 + Q4)$ of the second moments of the velocity-pressure interaction are shown for a channel flow with blowing. For the Couette flow, similar data were obtained.

Figures 3(a), 3(b), 3(c)and 3(d) show the two-point correlation between $v'$ and the instantaneous pressure gradient, $\nabla p'$, for a channel flow perturbed with blowing at $W^+$ from the slot and at $y^+ = 38$ from the wall, for the events at $Q2$ and $Q4$. These figures illustrate why the events at $(Q2 + Q4)$ are responsible for the increased wall-normal velocity-pressure interaction immediately downstream of the perturbation region.

The two-point correlation was evaluated for 21 instantaneous flow fields with $Pr = 1$ for a channel flow perturbed with blowing, which were equally separated in time $30(\nu/u_\tau^2)$. The expression for the two-point correlation coefficient is as follows:

$$R(r_x, y, r_z) = \langle A(x, y_d, z)B(x + r_x, y, z + r_z) \rangle, \tag{1}$$

where $(x, y_d, z)$ is the detection point and $(x+r_x, y, z+r_z)$ is the second point; $A$ is the first and $B$ the second variable (e.g., for $\langle v'\partial p'/\partial x \rangle$, $A = \partial p'(x, y_d, z)/\partial x$, $B = v'_x(x + r_x, y, z + r_z)$) and $\langle\ \rangle$ denotes averaging over $x$, $z$, and time.

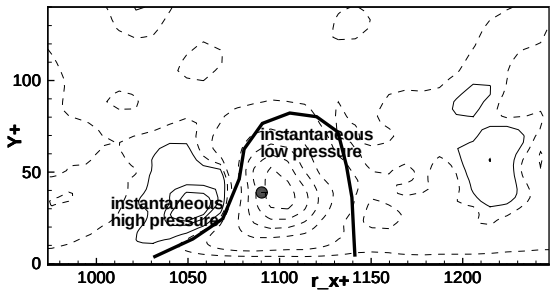


(a)

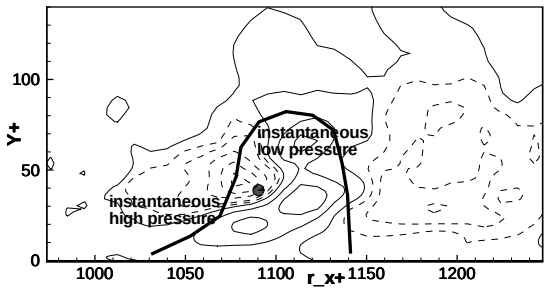


(b)

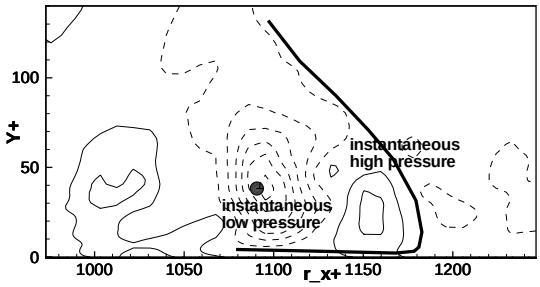


(c)

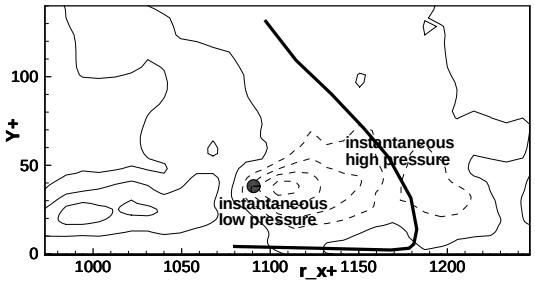


(d)

Figure 3: Two-point correlation for $\langle v'\partial p'/\partial x\rangle$(a-c) and $\langle v'\partial p'/\partial y\rangle$ (b-d) for channel flow perturbed with blowing, at $Q2$(a-b) and $Q4$(c-d) events, at $(r_x^+, y^+)$ plane ($r_z^+ = 0$). Contour levels are from $-0.06$ to $0.01$ with increments of $0.01$ for (a-c), and from $-0.04$ to $0.02$ with increments of $0.01$. Solid line, positive; dotted line, negative. Dots denote detection point $W^+$ from slot and at $y^+ = 38$ from the wall. Thick black lines denotes a possible region affected by $Q2$ or $Q4$ events.

Figure 3(a) shows $\langle v'(r_x, y, r_z)\partial p'(0, y_d, 0)/\partial x\rangle$ and 3(b) $\langle v'(r_x, y, r_z)\partial p'(0, y_d, 0)/\partial y\rangle$ for a $Q2$ event. Because an event at $Q2$ is a combination of $v' > 0$ with $u' < 0$, it can be thought of as the result of a mass of cold fluid with low axial momentum being raised up and brought into contact with hot fluid with a higher level of axial momentum (the combination of these low/high levels of momentum and heat is responsible for $u'$ and $\theta'$). Figure 3(a) shows that at the detection point, there is a region in which $\langle v'\partial p'/\partial x\rangle < 0$ and, upstream of it, a region where $\langle v'\partial p'/\partial x\rangle > 0$. Because $v' > 0$ for all $r_x^+$ and $y^+$ in this figure, in the first region, $\partial p'/\partial x < 0$, and in the second, $\partial p'/\partial x > 0$, revealing that when a mass of fluid with low axial momentum is raised up at $Q2$, it is surrounded with fluid with a higher level of axial momentum. Therefore, a region with a high instantaneous pressure is generated upstream, and an instantaneous favorable pressure gradient region is generated at the detection point and the next downstream region. As a consequence, we observe negative values of $\langle v'\partial p'/\partial x\rangle$ throughout the entire region occupied by this mass of fluid coming from the near-wall area, representing a source of $\langle v'u'\rangle$ or a defect in the turbulent axial momentum transferred in the $y$ direction. However, in contrast to $v'\partial p'/\partial x < 0$ (which is generated within the new region occupied by the mass of fluid that is raised up), according to Figure 3(b), $v'\partial p'/\partial y < 0$ is generated in the region upstream. In other words, both Figures 3(a) and 3(b) show that the instantaneous high-pressure field upstream of the mass with low axial momentum forms a sharp angle with the wall. Therefore, within this region upstream of the mass, $v'\partial p'/\partial y < 0$, representing a source of $\langle v'v'\rangle$ or a transfer of turbulent axial momentum in the $y$ direction (because $v' > 0$ and $\partial p'/\partial y < 0$, we have an instantaneous favorable pressure gradient). According to this analysis, the contribution of $v'\partial p'/\partial x < 0$ and $v'\partial p'/\partial y < 0$ at a single point does not occur simultaneously, as $\langle v'u'\rangle$ is generated within the mass of fluid that was raised up and $\langle v'v'\rangle$ is generated in the region upstream.

Following this argument, under developed conditions, this ascending mass of fluid should also create a region with low instantaneous pressure, mostly at its front and top region. In comparison with a perturbed flow, however, this mass has a higher level of axial momentum and heat; therefore, $u'$ and $\theta'$ should be lower than in a perturbed flow, and the contributions to the wall-normal velocity-pressure interaction should also be lower. The results showing these aspects of the phenomenon are being published elsewhere (Pasinato, 2011b).

Figure 3(c) shows $\langle v'(r_x, y, r_z)\partial p'(0, y_d, 0)/\partial x\rangle$ and 3(d) $\langle v'(r_x, y, r_z)\partial p'(0, y_d, 0)/\partial y\rangle$ for a $Q4$ event. A $Q4$ event can be thought as a mass of hot fluid with high axial momentum descending from the upstream part of the central region. Thus, coming into contact with cold fluid with low axial momentum, this mass creates a region with high instantaneous pressure, mostly at its front and top region, as shown in Figures 3(c) and 3(d). In contrast with developed conditions, however, in the perturbed region ($W^+$ downstream of the slot), it has an even higher instantaneous pressure (for a perturbed flow, the fluid near the wall has a lower axial momentum and less heat than in developed conditions). Thus, this $Q4$ event generates $\partial p'/\partial x > 0$ and $\partial p'/\partial y > 0$, and because $v' < 0$ throughout the whole region, $v'\partial p'/\partial y < 0$ and $v'\partial p'/\partial x < 0$ are sources of $\langle v'v'\rangle$ and $\langle u'v'\rangle$, respectively.

In other words, the generation of negative values of $\langle v'\partial p'/\partial y\rangle$ and $\langle v'\partial p'/\partial x\rangle$ also occurs in $(Q2 + Q4)$ events under developed conditions; however, in a perturbed region, there is a greater difference in the axial momentum and heat between the wall layer and the central region, which promotes the conditions at these events, generating even greater contributions from the correlations $\langle v'\partial p'/\partial y\rangle < 0$ and $\langle v'\partial p'/\partial x\rangle$ (note that Figures 2(a) and 2(b) show that the increase in the correlation between $v'$ and $\nabla p'$ coincides with the point at which the mean axial pressure gradient is slightly adverse).

The results presented above show that the dissimilarity between the axial and wall-normal turbulent fluxes of momentum and heat is the result of the same physical phenomenon responsible for the turbulent transport of momentum and heat in developed conditions, which was intensified by the perturbations, producing dissimilarity. As shown in Tables 2 and 3, most of the $\langle v'v' \rangle$ and $\langle u'u' \rangle$ second moments for the perturbed turbulence were generated in the ascending or descending events responsible for the generation of $\langle u'v' \rangle$, at almost the same percentage as that in the developed conditions. Similar results were observed for the turbulent heat fluxes $\langle \theta'v' \rangle$ and $\langle \theta'u' \rangle$ (results not shown here; Pasinato (2011b)).

Based on the above analysis, there are two fundamental aspects of dissimilarity that are worth noting (although they may be obvious and trivial) for the perturbed turbulent flow with heat transfer studied here. The first aspect is that the mean fields ($U$, $\Theta$, $P$) are always primarily responsible for the dissimilarity. Second, at the wall layer, $u'$, $v'$ and $\theta'$ (as in developed conditions) resulted from the exchange of momentum and heat occurring in that region due to the upward and downward movements of the turbulence between the wall and the central region.

Thus, if dimensional analysis is used to find an expression for $u_{rms}$ ($= \sqrt{(u')^2}$) and for $\theta_{rms}$ ($= \sqrt{(\theta')^2}$), these expressions should be a function first of $(dU/dy)$ and $(d\Theta/dy)$, respectively, and of $dP/dx$ and $dP/dy$, as the second moments $\langle v'\partial p'/\partial x \rangle$ and $\langle v'\partial p'/\partial y \rangle$ are indirect functions of the mean axial and wall-normal pressure gradients (where all the variables are non-dimensionalized using the wall variables $u_\tau$ and $\nu/u_\tau$ as in $y^+ = u_\tau y\rho/\nu$), as well as $y^+$, $Re_\tau$, and $Pr$, among others.

$$u_{rms} = K_1\{(\frac{\partial U}{\partial y})^a; (\frac{\partial U}{\partial x})^b; (\frac{\partial P}{\partial y})^c; (\frac{\partial P}{\partial x})^d; ...\} \tag{2}$$

and,

$$\theta_{rms} = K_2\{(\frac{\partial \Theta}{\partial y})^e; (\frac{\partial \Theta}{\partial x})^f; (\frac{\partial P}{\partial y})^g; (\frac{\partial P}{\partial x})^h; ...\} \tag{3}$$

Therefore, at least for the simple perturbed flow with heat transfer used here, the following relation can be proposed as a first approximation for the wall layer:

$$\frac{u_{rms}}{\partial U/\partial y} \simeq \frac{\theta_{rms}}{\partial \Theta/\partial y} \tag{4}$$

| | CHB6220 | CHABR220 | CFB6590 | CFABR590 |
|---|---|---|---|---|
| Non-perturbed | 0.79 | 0.79 | 0.78 | 0.78 |
| Middle of perturbation | 0.82 | 0.85 | 0.79 | 0.75 |
| $W^+$ from slot | 0.76 | 0.78 | 0.79 | 0.75 |
| $5W^+$ from slot | 0.75 | 0.78 | 0.78 | 0.75 |

Table 2: Ratio $\langle v'v' \rangle_{\langle u'v' \rangle < 0} / \langle v'v' \rangle$ at $y^+ = 38$.

Figures 4(a)-5(b) show these relations for non-perturbed and perturbed flows for channel and plane Couette flows. These figures clearly show that most of the dissimilarity between $u_{rms}$ and $\theta_{rms}$ can be explained by the wall-normal gradient of the mean fields. In the next section, the expression (4) is used to propose a strategy for modeling the turbulent heat flux at the wall layer.

| | CHB6220 | CHABR220 | CFB6590 | CFABR590 |
|---|---|---|---|---|
| Non-perturbed | 0.83 | 0.83 | 0.77 | 0.77 |
| Middle of perturbation | 0.79 | 0.78 | 0.78 | 0.73 |
| $W^+$ from slot | 0.80 | 0.76 | 0.80 | 0.72 |
| $5W^+$ from slot | 0.81 | 0.78 | 0.79 | 0.76 |

Table 3: Ratio $\langle u'u' \rangle_{\langle u'v' \rangle < 0} / \langle u'u' \rangle$ at $y^+ = 38$.

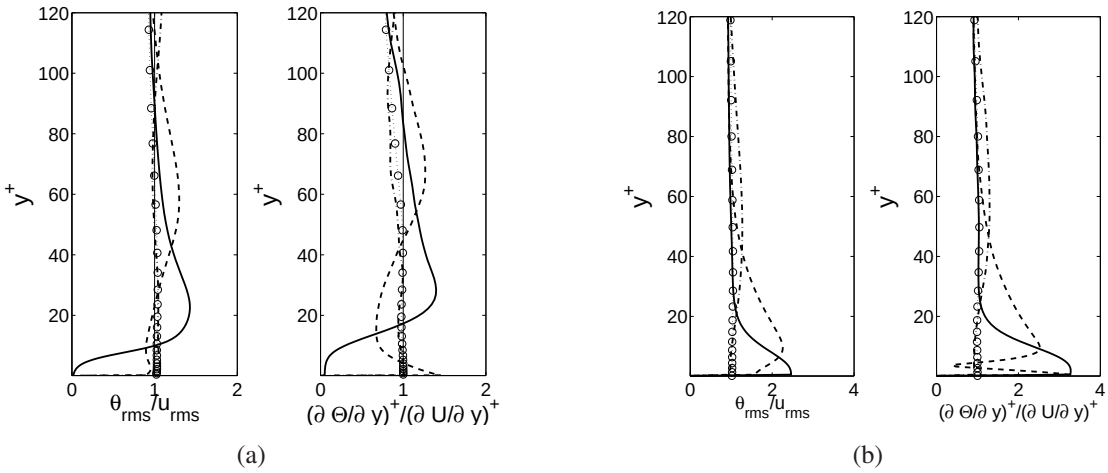


Figure 4: $\theta_{rms}/u_{rms}$ and $(\partial\Theta/\partial y)/(\partial U/\partial y)$ for channel flow perturbed with (a) blowing and (b) temperature step at the wall. $\circ \cdot \circ \cdot \circ$ , developed values. Solid line, on the slot; $- - -$, $W^+$; $-.-.-$, $5W^+$ downstream.

## 3 WALL-LAYER TURBULENT HEAT FLUX MODEL

The idea in this section is to present a strategy for modeling turbulent heat fluxes using the Reynolds stress in the $x - y$ plane. There are two reasons for this choice: (a)strong similarity exists between the axial turbulent momentum and heat in developed conditions, and (b) the wall-normal mean field gradients play a relevant role in dissimilarity. However, we must note that the proposal is not universal; it is only a good approximation for the wall layer (viscous, buffer and logarithmic layers). It is not appropriate for more isotropic flows or thermal fields at the central region.

The expression (4) and Figures 4(a)-5(b)) show that the rms of the fluctuations of axial velocity and temperature seems to be approximately related by the following:

$$\frac{\theta_{rms}}{u_{rms}} \simeq \frac{\partial\Theta/\partial y}{\partial U/\partial y} \tag{5}$$

Therefore, the following expressions are proposed to transform the Reynolds stress to turbulent heat fluxes:

$$\langle \theta' u' \rangle \simeq \langle u'u' \rangle \frac{\theta_{rms}}{u_{rms}} \simeq \langle u'u' \rangle \frac{\partial\Theta/\partial y}{\partial U/\partial y} \tag{6}$$

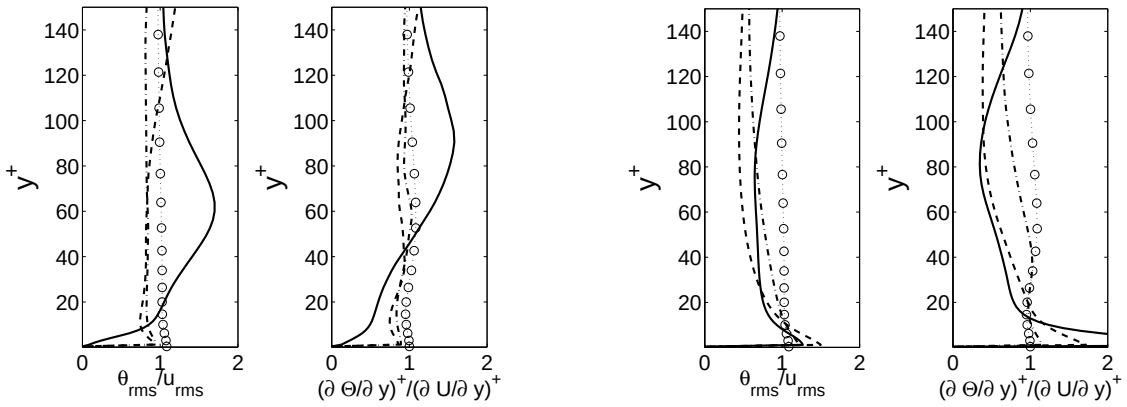


Figure 5: Idem Figures 4(a) and 4(b) for Couette flow perturbed with (a) blowing and (b) adverse axial pressure gradient step.

and,

$$\langle \theta' v' \rangle \simeq \langle u' v' \rangle \frac{\theta_{rms}}{u_{rms}} \simeq \langle u' v' \rangle \frac{\partial \Theta / \partial y}{\partial U / \partial y} \tag{7}$$

Note that expression (7) for the wall-normal turbulent heat flux matches the expression for $\langle \theta' v' \rangle$ when $Pr_t = 1$ is used with the standard gradient-diffusion hypothesis. In other words, the first results extracted from the simple perturbed turbulent flow with heat transfer used in this study express that, at least for $Pr = 1$, the turbulent heat flux in the wall-normal direction is modeled well by using the standard gradient-diffusion hypothesis. Conversely, expression (6) implies that this is not the case for the axial turbulent heat flux. A complete analysis of the previous proposal will be published elsewhere (Pasinato, 2011b).

Figures 6(a)-7(b) show an *a priori* comparison of the partial model for expressions (6-7). These figures show that the channel flow is better modeled than the Couette flow. For the channel flow, the worst *a priori* predictions are for $\langle \theta' v' \rangle$ for the adverse pressure gradient step, through the logarithmic region for $50 < y^+ < 100$ on the slot and $W^+$ downstream (this region is immediately outside the buffer region, where the pressure-gradient step was applied) as well as $\langle \theta' u' \rangle$ for the adverse pressure gradient step at $W^+$ downstream, for $5 < y^+ < 50$. For the Couette flow, the worst prediction is for $\langle \theta' v' \rangle$ at the slot for blowing, and for the adverse pressure gradient step, the worse prediction is mainly in the logarithmic region.

## 4 CONCLUSIONS

In this work, expressions for the turbulent heat fluxes $\langle \theta' u' \rangle$ and $\langle \theta' v' \rangle$ in the wall layer are proposed based on the fluxes of the axial turbulent momentum $\langle u' u' \rangle$ and $\langle u' v' \rangle$ and the wall-normal gradients of the mean fields $U$ and $\Theta$. A pre-generated database obtained from DNS of perturbed turbulent channel and plane Couette flows with heat transfer was used. The main conclusions of this work are as follows.

According to previous results on dissimilarity (Pasinato, 2011a; Pasinato and Squires, 2011) and the present work, the dissimilarity between the wall-normal gradients of $U$ and $\Theta$ (as a consequence of the mean axial pressure gradient) is primarily responsible for the dissimilarity between the Reynolds stress and turbulent heat flux, and between $u'$ and $\theta'$ itself, for the flow

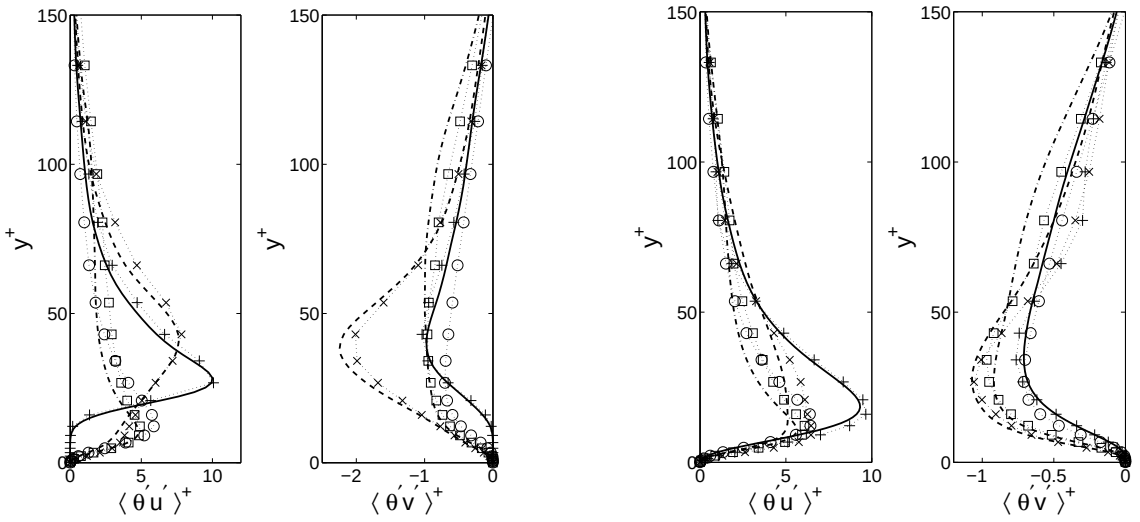


Figure 6: *A prior* comparison of modeled turbulent heat flux $\langle\theta' u'\rangle^+$ and $\langle\theta' v'\rangle^+$, for channel flow perturbed with (a) blowing and (b) an adverse axial pressure gradient step. Solid line, and $+\cdot+\cdot+$(second symbol modeled), on the slot; $-\,-\,-$, and $\times\cdot\times\cdot\times$ , $W^+$; $-.\,-\,.-$, and $\square\cdot\square\cdot\square, 5W^+$ downstream; $\circ\cdot\circ\cdot\circ$ , non-perturbed values.

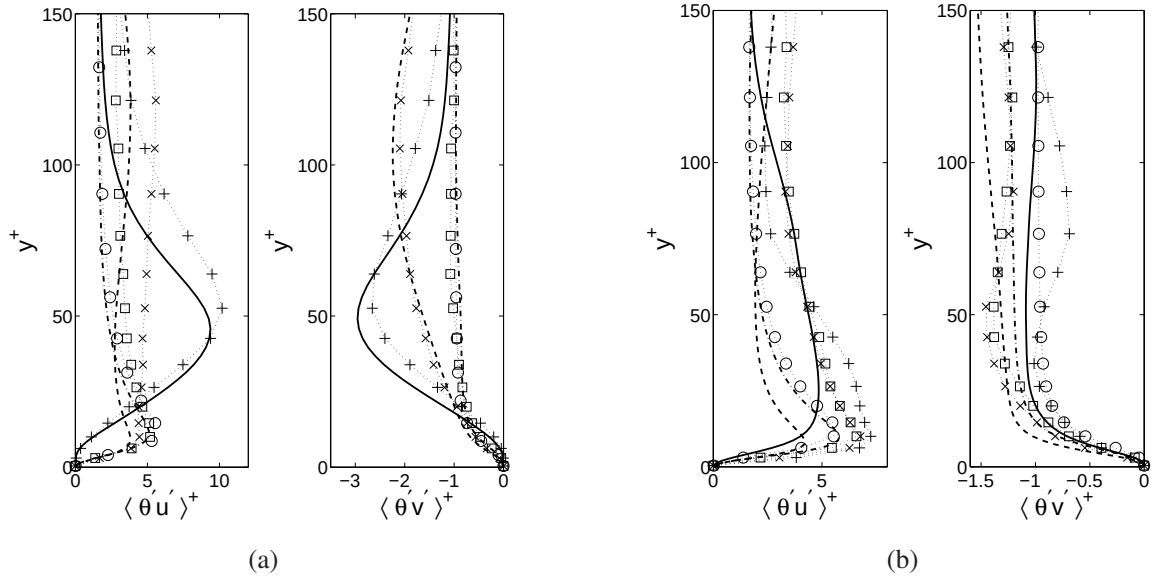


Figure 7: Idem Figures 6(a) and 6(b) for Couette flow. (a) blowing, (b) adverse axial pressure gradient step.

studied here.

The expressions $\theta_{rms}/u_{rms} \simeq (\partial\Theta/\partial y)/(\partial U/\partial y)$ approximately hold for the simple perturbed flow studied here.

The gradients $(\partial\Theta/\partial y)$ and $(\partial U/\partial y)$ can be used to transform the axial turbulent fluxes $\langle u'u'\rangle$ and $\langle u'v'\rangle$ to express the heat fluxes $\langle\theta'u'\rangle$ and $\langle\theta'v'\rangle$.

Although the transformation of the Reynolds stresses in the $x-y$ plane using the wall-normal gradient of the axial velocity and temperature is only an approximation, it performs reasonably well as a partial model of the turbulent heat fluxes for the perturbed turbulent flows used here. Most importantly, it shows that an important part of the dissimilarity between the Reynolds stress and the heat flux can be modeled using only information from the mean field dissimilarity.

Furthermore, the axial turbulent fluxes seem to be more related to the wall-normal gradients of the mean fields than to the axial gradients. Therefore, this result contradicts both the standard and the generalized gradient-diffusion hypothesis for the axial turbulent heat flux.

The *a priori* comparisons of the turbulent heat fluxes transformed with $(\partial\Theta/\partial y)/(\partial U/\partial y)$ presented a reasonable behavior for the perturbed flow with heat transfer used here.

## REFERENCES


Abe K. and K. Suga, Towards the development of a Reynolds-averaged algebraic turbulent scalar-flux model, *Int. J. Heat Fluid Flow* 22:19-29, 2001.

Daly, B.J. and F.H. Harlow. Transport equations in turbulence, *Physics of Fluid*, 13:2634-2649, 1970.

Qiu, J.F.; S. Obi and T.B Gatski, On the wake-equilibrium condition for derivation of algebraic heat flux model, *Int. J. Heat Fluid Flow*, 29:1628-1637, 2008.

Houra, T. and Y. Nagano Effects of adverse pressure gradient on heat transfer mechanism in thermal boundary layer. *Int. J. of Heat and Fluid Flow*, 967-976, 2006.

Kasagi, N. and M. Nishimura, Direct numerical simulation of combined forced and natural turbulent convection in a vertical plane channel, *Int. J Heat Fluid Flow*, 18:88-90, 1997.

Kim, J. and P. Moin. Transport of Passive Scalar in a Turbulent Channel Flow. In *Turbulent Shear Flow*, 6:86-96, 1989.

Kong, H., H. Choi, and J.S. Lee.Dissimilarity between the velocity and temperature fields in a perturbed turbulent thermal boundary layer. *Physics of Fluids*, 13:5:1466-1479, 2001.

Lyons, S.L, Hanratty, T.J. and Mclaughlin J.B.*Direct numerical simulation of passive heat transfer in a turbulent channel flow*, *Int. J. Heat Mass Flow*, 34:1149-1161, 1991.

Pasinato, H.D. Velocity and Temperature Dissimilarity in Fully Developed Turbulent Channel and Plane Couette Flows, *Int. J. Heat and Fluid Flow*, 32:11-25, 2011.

Pasinato, H.D. and K.D. Squires. Axial Velocity and Temperature Dissimilarity in Perturbed Turbulent Channel and Plane Couette Flows, sub. to *Int. J. Heat and Fluid Flow*.

Pasinato, H.D. Wall layer turbulent heat transfer model, to be submitted.

Rossi, R. and G. Iaccarino. Numerical simulation of scalar dispersion downstream of a square obstacle using gradient-transport type models, *Atmospheric Environment*, 1-14, in press.

Rossi, R. A numerical study of algebraic flux models for heat and mass transport simulation in complex flows. *Int. J. Heat Mass Trans.*, 53:4511-4524, 2010.

Suzuki, H., K. Suzuki, and T. Sato. Dissimilarity between heat and mass transfer in a turbulent boundary layer disturbed by a cylinder. *Int. J. Heat Mass Transfer*, 31:2:259-265, 1988.

Suzuki, K., and K. Inaoka. Flow modification and heat transfer enhancement with vortices. *Int. J. Transport Phenomena*, 1:17-30, 1998.